

Article

# Assessment of Wave Storm-Induced Flood Vulnerability in Rhodes Island, Greece

Fragkiska-Karmela Gad <sup>\*</sup>, Maria Chatzinaki, Dimitris Vandarakis , Chara Kyriakidou and Vasilios Kapsimalis

Institute of Oceanography, Hellenic Centre for Marine Research (HCMR), 19013 Anavyssos P.C., Greece; marhatz@hcmr.gr (M.C.); divandarakis@hcmr.gr (D.V.); hkyriakid@hcmr.gr (C.K.); kapsim@hcmr.gr (V.K.)

\* Correspondence: fgad@hcmr.gr; Tel.: +30-229-107-6378

Received: 31 August 2020; Accepted: 20 October 2020; Published: 23 October 2020



**Abstract:** Coastal areas are threatened by extreme meteorological phenomena, such as wave storms. Therefore, the analysis of such events, such as providing information for their potential hazards assessment, is a key element in coastal management. In this study, a preliminary assessment of flood vulnerability due to storms was performed in Rhodes Island, Greece. Firstly, storm events were defined in terms of significant wave height, peak period, and duration, and they were grouped by means of cluster analysis into five classes (from weak to extreme) reflecting the intensity of each event. Subsequently, flood hazard was assessed by using an empirical formula for wave run-up calculations on cross-shore profiles and storm surge data at the region. Finally, a Flood Vulnerability Index (FVI) was used for assessing vulnerability according to a scale from very low to very high. The most intense storms were found to occur in the eastern, southeastern, and southern part of the island. More than 60% of storms were classified as weak, while extreme events were found to occur with a frequency of less than 2.5%. Regarding flood hazard and vulnerability, the maximum values of wave run-up were calculated in the southeastern region, but the most vulnerable part was found to be the northwestern region, as the FVI was assessed as very high for weak and extreme events.

**Keywords:** wave storms; run-up; storm surge; coastal flooding; Flood Vulnerability Index; Aegean Sea

## 1. Introduction

Coastal areas are highly dynamic systems that are affected by several forcing factors. Extreme wave storms cause significant socio-economic and environmental impacts on coastal areas such as human lives lost, the degradation of biodiversity, and damages to infrastructure and properties [1–7].

The intensity of storm-induced coastal processes and the morphodynamic response of a coastal area to an extreme storm event strongly depend on the characteristics of the storm (e.g., storm peak, duration, directionality, and energetic content), as well as on the characteristics of the coastal area (e.g., beach profile, gain size, and relative orientation of the shoreline) [2,3].

Thus, the analysis of such events and the assessment of their impact are key elements in coastal management and planning, providing a tool to stakeholders and decision makers for selecting the best mitigation and adaptation measures to protect affected areas. The necessity of potential hazard prevention is highlighted in the Protocol on Integrated Coastal Zone Management in the Mediterranean [8] and in the EU Floods Directive 2007/60/EC, which indicate regulations for the assessment and management of flood hazards.

The assessment of flood vulnerability in a specific coastal region requires an extensive analysis of a wave climate. In particular, the consideration of vulnerability due to wave storms demands the identification of the intensity and duration of each storm event. Dolan and Davis [9,10] firstly proposed a storm classification into five categories—I: weak; II: moderate; III: significant; IV: severe;

and V: extreme—in terms of their released energy, which is expressed by wave height and the duration of storms.

Wave storms usually cause coastal floods as a result of wave run-up and storm surge [11]. Wave run-up is considered as an important parameter for engineers and decision makers when defining the landward boundary of a coast [12]. There are several empirical formulas [13–15] and numerical models [16–18] for estimating wave run-up that depend on both wave parameters and coastal geomorphology. The selection of an appropriate method for evaluating wave run-up depends on the spatial scale of the analysis (i.e., local, regional, or global) and the available data. On the other hand, storm surge is estimated by numerical models [19,20]. Recently, Mendoza and Jimenez [21] developed the Flood Vulnerability Index (FVI) to assess the potential coastal flood hazard based on wave run-up, storm surge, and beach morphology (e.g., beach height). The FVI is sorted into five classes ranging from very low to very high.

In this context, the present study provides a preliminary evaluation of flood vulnerability at a regional scale based on (a) the analysis of wave storm events; (b) the assessment of potential flood hazard, which was parameterized by using wave run-up and surge during storm events; and (c) the calculation of the FVI in Rhodes Island, Greece. The study area is a mass touristic destination, and such an analysis is therefore of essential interest for the local community. The same approach has also been applied in several regions of different spatial scales such as the Atlantic coast [9,22,23] and the Mediterranean Sea [5,24–26] for estimating coastal vulnerability to potential flood hazard.

## 2. The Study Area

Rhodes Island, located in the Dodecanese insular complex in the southeastern Aegean Sea (Figure 1), is the fourth largest island in Greece, with a total surface area of 1400 km<sup>2</sup> and a coastline length of 253 km. According to the 2011 census, it has a permanent population of 115,490 inhabitants. The island is of high interest due to its high population density and significant tourism activities, particularly in its north-northwestern, north-northeastern, and eastern parts.

The beaches of Rhodes have a 7–8% slope in the northern part, and they are gentler (a slope of about 4%) in northwest part of the island [27]. The beaches in northeastern part have a mean slope of about 6%, which is steeper in the eastern, southeastern, and southwestern (about 7%) regions. In the central west part, cliffs predominate and the few sandy beaches have a mean slope of greater than 15%.

The analysis revealed that prevailing winds in the region blow from west, west-northwest, and west-southwest. However, the strongest events come from southeast and east-southeast, with speed values exceeding 15 m/s. In regard to the wave conditions, the dominant propagation directions are the west, west-southwest, and west-northwest, with a frequency of occurrence of more than 25%. At the northern and eastern part of the island, the highest waves come from south-southeast and south-southwest, while at the southern and western parts, the strongest events propagate from west-northwest and west. In the southern regions, when strong winds blow over long fetches, the significant wave height can exceed 6.5 m, while in north, the wave height can reach up to 4.3 m. Wind-generated waves are the most common type in the study area, with normal peak wave period values ranging from 3 to 6 s. Only a very small percentage of wave events (<0.01%) are swells with a peak wave period of greater than 15 s.

The micro-tidal regime of the area of Rhodes Island extends from 0.1 to 0.36 m, with a mean value of 0.14 m during 2010–2012.

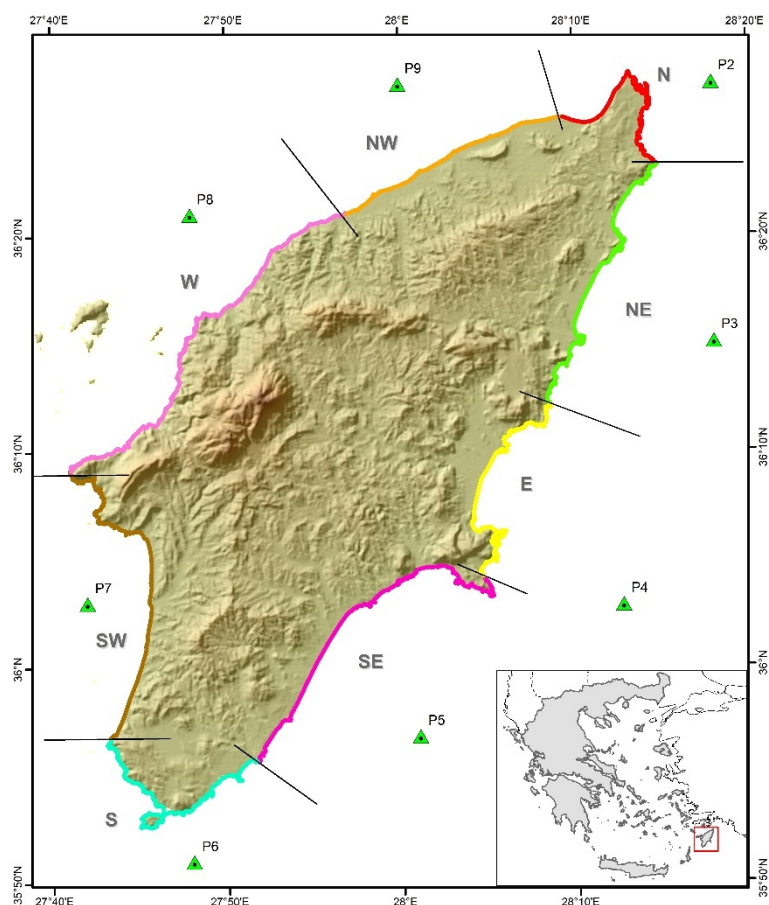


**Figure 1.** Rhodes Island, Greece, and the locations of data points and geographical parts of the island used for the analysis of storm events.

### 3. Materials and Methods

#### 3.1. Data

The wave data used for the analysis were derived from the “Wind and Wave Atlas of the Hellenic Seas” (hereafter “Atlas”) managed by Hellenic Centre for Marine Research (HCMR) [28], a high spatial ( $0.1^\circ \times 0.1^\circ$ ) and temporal (3 h) resolution hindcast analysis covering a 10-year time period (1995–2004). The time series data of significant wave height ( $H_s$ ), peak wave period ( $T_p$ ), and mean wave direction (MWD) were extracted at 9 offshore locations (Figure 1).

In addition, water level data resulting from storm surge were acquired from the Copernicus database that includes time series of historical data and predictions about future events (up to 2100) in a high spatial ( $0.1^\circ \times 0.1^\circ$  in the coastal zone and up to  $1^\circ \times 1^\circ$  offshore) and temporal (10 min) resolution analysis [29].

Bathymetric data were provided by the HCMR and European Marine Observation and Data Network (EMODnet) databases [30], while topographic data were provided by the Hellenic Cadastre.

#### 3.2. Analysis of Wave Storms

In the international literature, a wave storm event is defined in terms of wave height and its duration. In this study, a storm was defined as an event in which significant wave height ( $H_s$ ) exceeded the 95th percentile of the data set [31,32] with a minimum duration of 6 h [24,33]. In addition, the time period between two consecutive storms was considered more than 24 h in order to identify statistically independent events [22]. Thus, two storms with an inter-event period shorter than 24 h were considered as one event with two peaks (Figure 2). An extra criterion taken into consideration was the mean

direction of storms in relation to coastline orientation; therefore, only the events that propagated towards the beaches of study area were included in the analysis. In particular, the mean direction of storms was calculated by applying circular statistics [34].

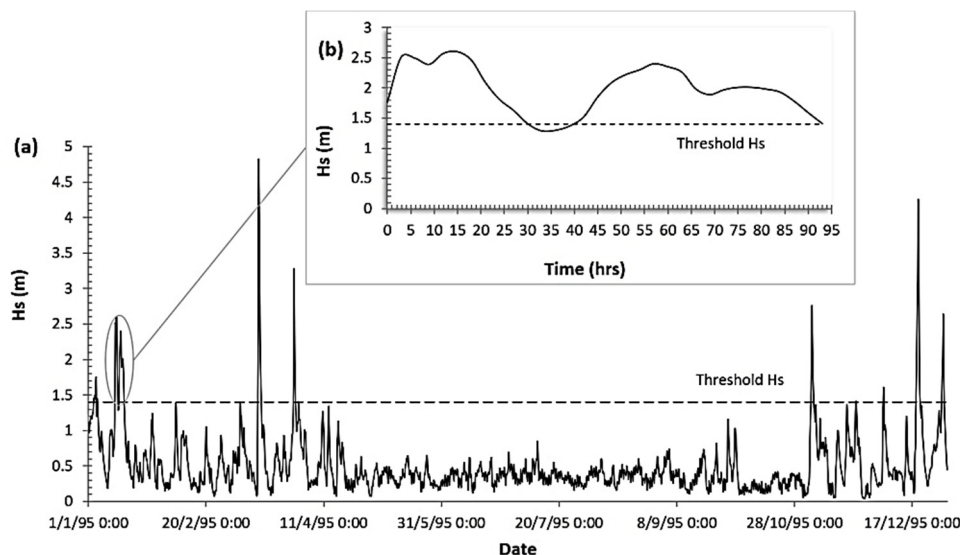


**Figure 2.** Time series of significant wave height (corresponding to the dataset of Atlas point P4) during (a) one year of the analysis (1995) and (b) a double-peaked storm event with  $H_s > 1.4$  m (threshold),  $dt = 93$  h, and inter-storm period = 9 h.

After identifying storm events in time series data, the parameters that reflect storm intensity were selected for the classification of storms into 5 groups by means of cluster analysis; namely, the average wave peak period ( $T_p$ ) of each event and its energy content ( $E$ ) [26]. The energy content ( $E$ ) of a storm event was expressed by Dolan and Davis [9,10] as:

$$E = \int_{t_1}^{t_2} H_s^2 dt \quad (1)$$

where  $H_s$  is the significant wave height and  $dt = t_2 - t_1$  is the storm duration.

More specifically, the hierarchical agglomerative cluster analysis was carried out with both average Linkage and Ward's methods by using the Euclidean distance between two variables ( $E$  and  $T_p$ ). These methods use different algorithms (with different weighting factors) to calculate the distance between two objects or groups [35]. Subsequently, Dunn and Silhouette indices were calculated to validate the above methods [26]. The first option of analysis defines clusters' density and how well-separated they are (its value is maximized for the best clustering method). The latter approach specifies the confidence degree of a cluster (a value close to one indicates well-clustered data). In this study, the optimum clustering approach was the average Linkage method, which has been also used in previous climate studies [9,10,24].

The consideration of the variations in wave climate due to differences in coastal morphology and orientation around the island was carried out by using data from 9 offshore locations, as presented in Figure 1.

### 3.3. Flood Hazard Assessment

The potential flood hazard was assessed by calculating the wave run-up on representative cross-shore profiles along the study area by the empirical formula of Stockdon et al. [15]:

$$R = 1.1 \left\{ 0.35\beta_f \sqrt{H_0 L_0} + \frac{1}{2} \left[ H_0 L_0 (0.563\beta_f^2 + 0.004) \right]^{1/2} \right\} \quad (2)$$

where  $\beta_f$  is the shoreface slope and  $H_0$  and  $L_0$  are the deep-water wave height and length, respectively, corresponding to the most intense conditions during a storm event. The above formula was selected because it can be used for dissipative (beaches characterized by gentle slope and fine sediments and subjected to high waves) and reflective (characterized by steep slope and coarse sediments and subjected to swells) beaches. The Iribarren number, a nondimensional parameter relating wave characteristics and beach slope that is associated with morphodynamic conditions, is defined as:

$$\xi_0 = \frac{\beta_f}{\sqrt{H_0 L_0}} \quad (3)$$

Low values of the Iribarren number (i.e.,  $\xi_0 < 0.3$ ) indicate dissipative conditions, and higher values indicate intermediate-to-reflective conditions [12].

Subsequently, the maximum wave run-up was calculated for each identified storm event at each profile. Moreover, a representative value of wave run-up was estimated for each class as the average of maximum values per storm event [24].

### 3.4. Flood Vulnerability Index

The Flood Vulnerability Index (FVI) is generally assessed based on wave run-up ( $R$ ), storm surge ( $\xi$ ), and maximum beach height ( $B_{max}$ ), and it is parameterized by an intermediate index, namely the Flood Intermediate Parameter (FIP) [21]:

$$FIP = \frac{R + \xi}{B_{max}} \quad (4)$$

The FVI is classified in 5 classes that extend from very low to very high vulnerability, and it is estimated following the functional rule shown in Figure 3, as proposed by Mendoza and Jimenez [21]. Thus, if total water levels during a storm event (wave run-up plus surge) are less than half of the beach elevation, then the flood vulnerability is defined as very low. When storm water levels (wave run-up plus surge) exceed the beach berm, then the flood vulnerability is very high.

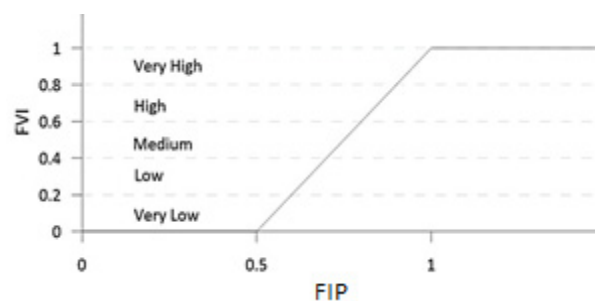


**Figure 3.** Assessment of the Flood Vulnerability Index (FVI) as a function of the flood intermediate parameter (FIP) [21].

## 4. Results

### 4.1. Analysis of Wave Storm Events

The above methodology was applied in eight geographical sections of Rhodes Island, which are presented in Figure 1, in order to classify storm events into five classes depending on their intensity (I—weak; II—moderate; III—significant; IV—severe; and V—extreme) and assess flood hazard and vulnerability in each region.

As mentioned above, the threshold value of wave height for defining a storm depends on the 95th percentile of the data set. Thus, the threshold value of significant wave height was found to vary with the geographical regions of the study area due to spatial variations in the wave climate, ranging from 1.25 m at the northern region of the island up to 2.0 m in the southern region. The increase of  $H_s$  threshold at the southern part of the study area was due to the most extreme wave conditions that propagate from the southeast sector.

The analysis revealed that the majority of the storms occur in the southern and western part of the island. More than half of the events (frequency of occurrence of >60%) were classified as weak (Class I), while extreme storms (Class V) were found to occur with a frequency of less than 2.5%. Figure 4 presents frequency of occurrence of storm classes in each geographical region of the island.

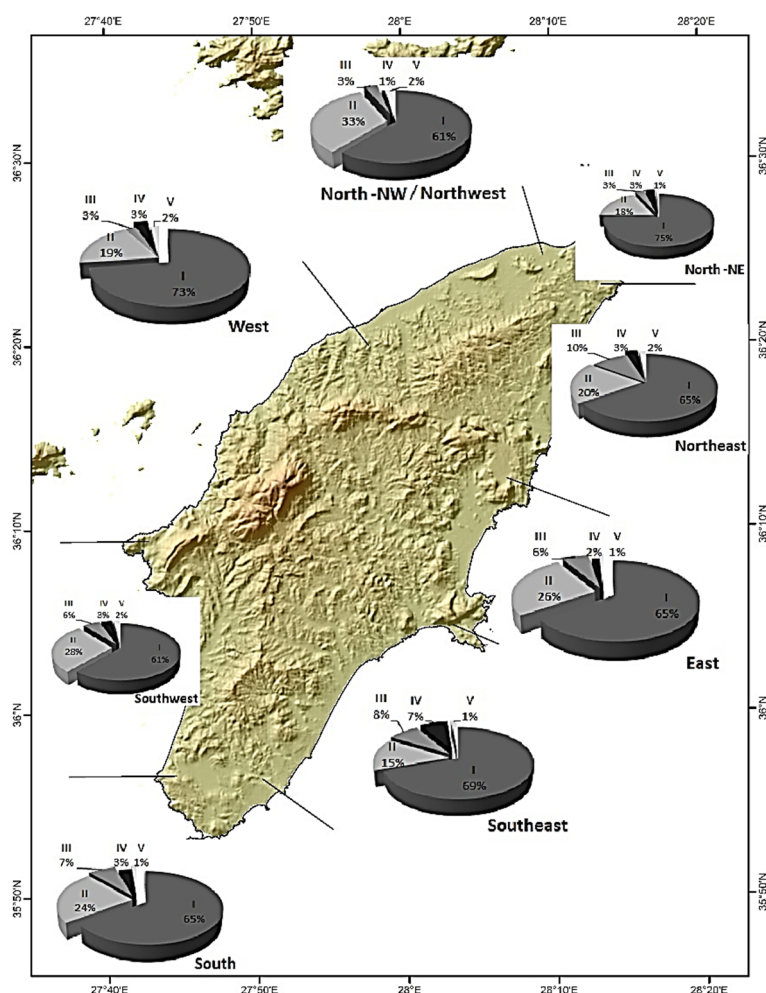


**Figure 4.** Frequency of occurrence of storm classes in each geographical region of the island.

Storm characteristics (i.e., wave height, wave period, energy, and duration) were found to generally increase as the intensity of storm events increased (Figures 5 and 6). Regarding wave characteristics (i.e., significant height and peak period) during weak storms, the mean value of the wave height ranged

from 1.4 m in the north-northwestern region up to 2.3 m in the southern region. During extreme storms, the maximum value of significant wave height was found to exceed 4.0 m and reached up to 6.6 m in the southern part of the island, whilst the mean significant wave height ranged from 2.0 m in the north-northwestern region up to 3.3 m in the southern region. The mean wave height increased from weak (Class I) to extreme (Class V) events by about 1.3–1.7 times. The average value of the wave peak period during weak storms ranged from 6.7 s in the northeast up to 7.9 s in the west, whilst during extreme events, it lied between 8.0 s (in the east) and 9.5 s (in the west). The mean value of the peak period increased from weak to extreme wave storms by about 1.2–1.3 times.

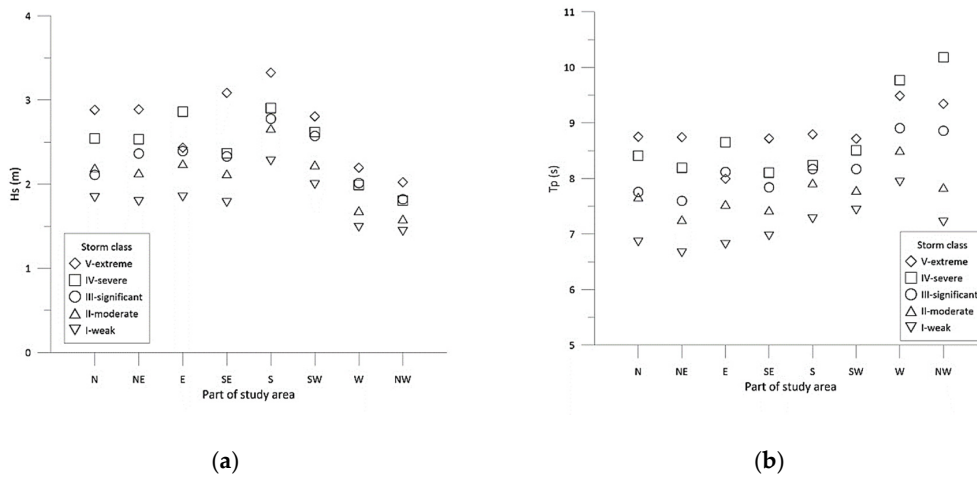


Figure 5. Average (a) significant wave height and (b) peak period for each storm class per geographical section of study area.

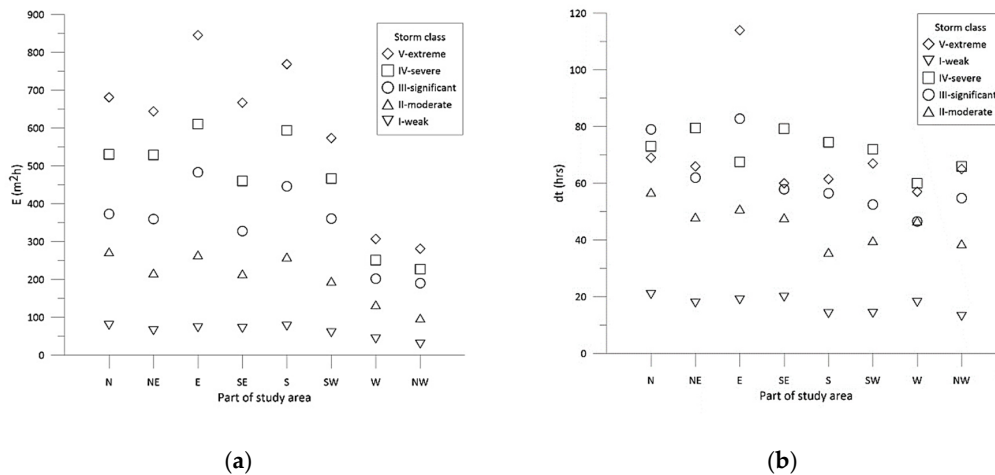


Figure 6. Average (a) wave energy and (b) duration for each storm class per geographical section of study area.

The analysis revealed that the energy content increased from weak (Class I) to extreme (Class V) events by about 7–12 times. The most intense storms were found to occur in the eastern, southeastern, and southern regions (with a mean energy content of more than 660 m<sup>2</sup> h); this was also where the greatest values of H<sub>s</sub> were recorded. The storm energy at the western and northwestern parts of the study area was about 30–60% of the energy content of the storms in the east and south. The wave energy during extreme events in west and northwest was found that it did not exceed 335 m<sup>2</sup> h. The mean duration of weak events did not exceed 21 h. The mean duration of extreme storms ranged from 60 to 114 h, with the greatest value corresponding to the eastern part of the study area. Figures 5

and 6 present the average values of storm characteristics for each class per geographical section of the island.

Regarding event direction, wave storms were found to mostly propagate from the southeast and south sectors in the northeastern, eastern, and southeastern regions, as well as from the west and southwest sectors in the south, southwest, west, and northwest regions.

#### 4.2. Assessment of Flood Vulnerability

##### 4.2.1. Results of Wave Run-up

Coastal flood vulnerability was assessed in terms of wave run-up and maximum beach height. Thus, a total of 62 cross-shore profiles were selected along the coastline of the island in order to calculate the maximum wave run-up during storm events. The location of each cross-shore profile per geographical sector is presented in Figure 7. The selected profiles extended from  $-25.0$  m to the land boundary of each beach zone (which reached up to  $+5.60$  m above the mean sea level (msl), depending on beach morphology at each profile). The distance between consecutive cross-shore profiles ranged from about 300 m at the northern headland up to 1000 m in the northwestern part of the study area, which is of great interest due to the area's high population density and concentration of economic activities, such as tourism [36]. In the northeast, east, and southeast, the distance between the profiles ranged from 500 to 5000 m. Only six profiles were selected in the southwest and west regions, where cliffs predominate and the area is underpopulated.

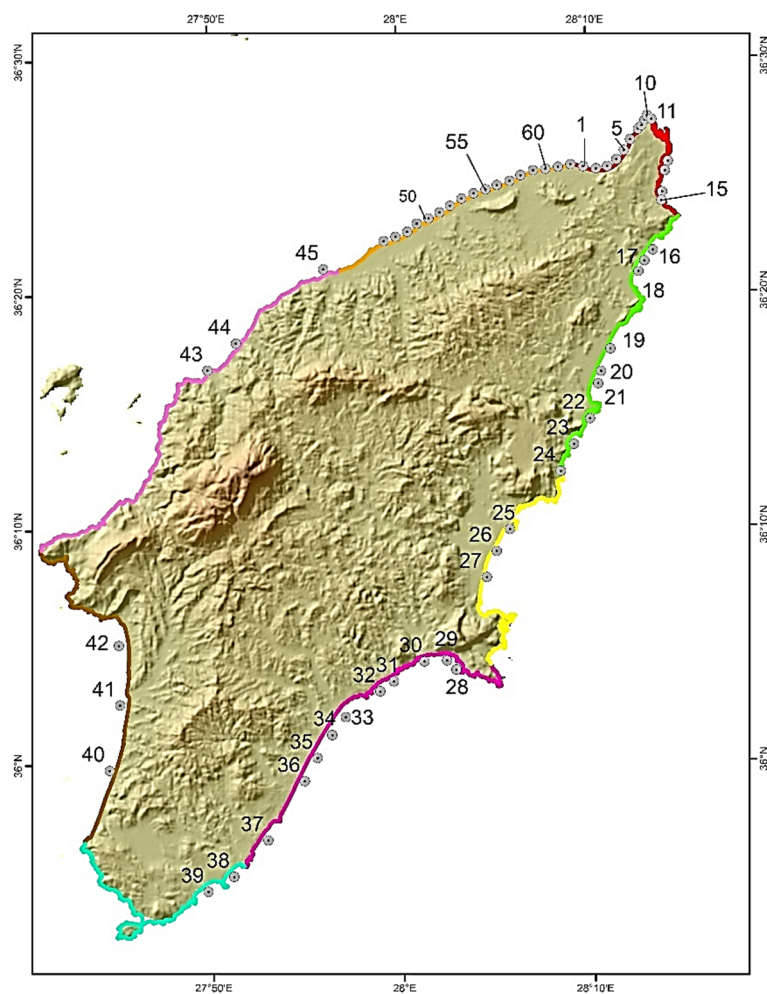


Figure 7. Locations of cross-shore profiles along the island.

Wave run-up was found to generally increase as the intensity of the storm events increased. Particularly, wave run-up during extreme storm events (Class V) was increased by 1.6–2.4 times relative to weak storms (Class I). The highest increase was estimated in the southeastern and southern regions, where the most intense events occur. The maximum wave run-up occurring during weak events (Class I) ranged from 0.8 to 5.5 m, whereas the representative values of run-up (i.e., the average of maximum values) ranged from 0.5 to 3.5 m. During extreme storms (Class V), the representative wave run-up reached up to 6.7 m. Moreover, for a specific storm event, the greatest wave run-up was found to occur on beach profiles with steeper slopes. Thus, the minimum values of wave run-up were calculated at the northern, northeastern, and northwestern parts of the island, associated with mild beach face slopes (<4%) under dissipative conditions (with a low Iribarren number,  $\xi_0 < 0.3$ ). The representative values of wave run-up for five storm classes and the morphology parameters of each profile are presented in Figure 8.

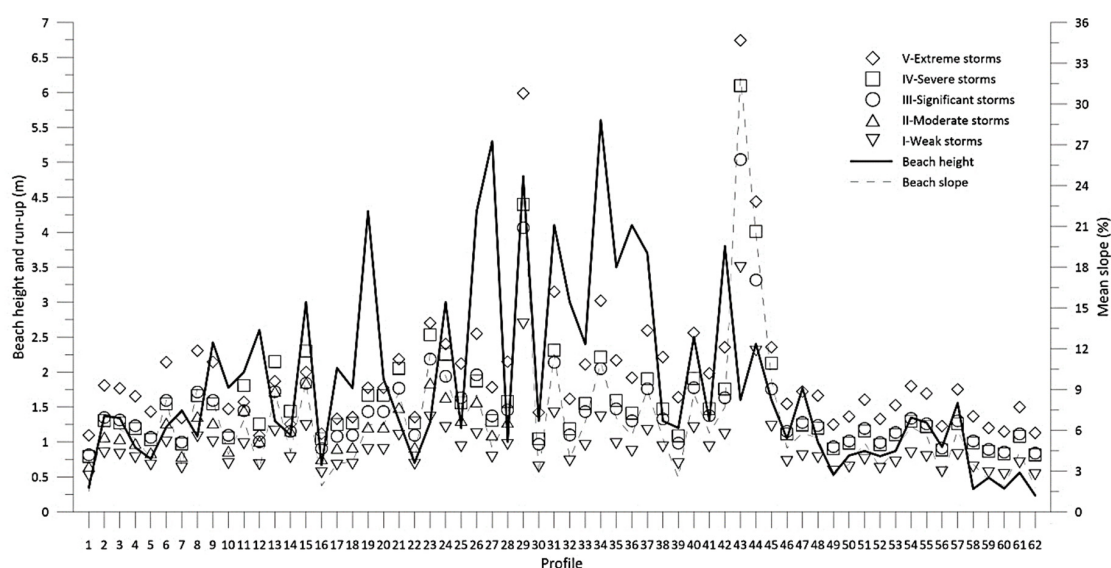


Figure 8. Morphological characteristics of cross-shore profiles and mean wave run-up per storm class.

#### 4.2.2. Storm Surge during Storm Events

The time series of storm surge were acquired from the Copernicus database for the analysis period. Both the maximum and the average values of storm surge were calculated during each storm event. A low correlation between storm surge and significant wave height was estimated over the analysis period at the western part of the study area, as the correlation coefficient was found to lie between 0.081 and 0.086; at the eastern part of Rhodes, the correlation coefficient between storm surge and significant wave height was calculated to range from 0.135 and 0.181. The maximum storm surge of each storm class was taken into account for calculating the FIP index to represent the worst-case scenario.

#### 4.2.3. Results of Flood Vulnerability Index (FVI)

Regarding the FVI, during weak storms, the vulnerability was assessed as very low at 29% of the examined profiles, low at 10%, medium at 3%, high at 8%, and very high at 50%. The southeastern region was found to be the least threatened by flooding hazard, although the most intense events were found to occur at this part of the study area due to strong south-east waves. On the other hand, the northwestern region (e.g., Kremasti, represented by profiles 58–62) with mild slopes, exposed to less intense storms propagating from west sector, presents a threat to flood during weak storms because wave run-up may exceed beach berm elevation during an event.

During extreme events, the FVI was assessed as very high over a significant part of the study area (about 76% of the selected profiles). Flood vulnerability was assessed as very low and low at about 12%

of the selected cross-shore profiles, mainly in the southeastern part of the island. The spatial variation of the FVI for weak and extreme events is presented in Figure 9.

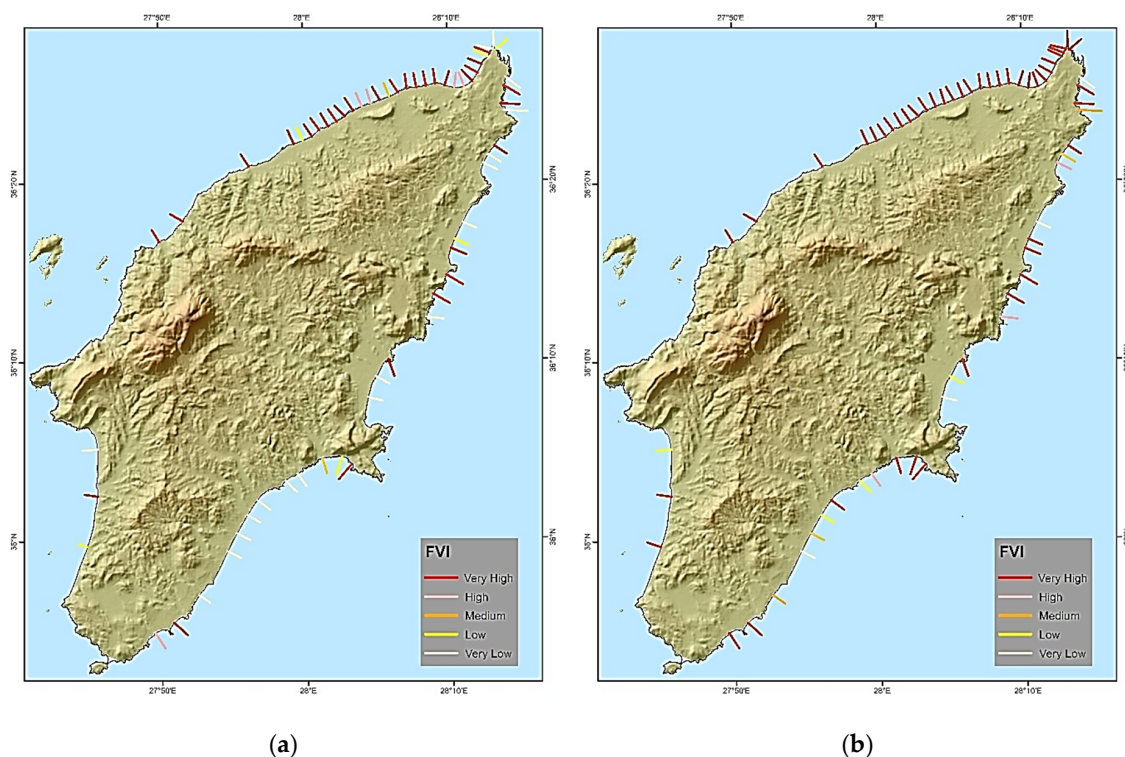


**Figure 9.** Spatial variation of the Flood Vulnerability Index in Rhodes Island for (a) weak (class I) and (b) extreme (class V) wave storms.

The FVI may significantly vary between successive profiles of a particular beach due to fluctuations in berm height. For instance, in the south-eastern part of the study area (Figure 1), the FVI was found to range from very high to very low among profiles 33–36 because the berm height highly varies due to the presence of uplifted beach rocks located at the backshore.

## 5. Discussion

The application of the above methodology to eight geographical sectors of Rhodes Island revealed the differences in coastal geomorphology and wave climate between these sectors. The threshold value of significant wave height for defining storms varied with the geographical regions of the study area due to spatial variations in the wave climate.

The optimum clustering approach for wave storm classification in Rhodes is the average Linkage method, which has been also used in previous studies of storm events in Atlantic coast [9,10] and in the Mediterranean Sea [37]. As the classification of storm events depends on their intensity, upper classes correspond to greater values of energy content. The number of events decreases to upper classes as more extreme events occur less often. Conversely, here, there was an increasing trend in values of storm characteristics (i.e.,  $H_s$ ,  $T_p$ , and  $dt$ ), as storm intensity increased. This trend was also found by Mendoza et al. [24] and Tsoukala et al. [5] in different sites in the Mediterranean Sea. In some cases, the average values of storm characteristics may be smaller in upper classes compared with corresponding values in lower classes, as an event may occur for a long period with small values of wave parameters, or vice versa, as Tsoukala et al. [5] also noted.

It was expected that wave run-up would generally increase as the intensity of storm events increased. Representative wave run-up values corresponding to extreme storms (Class V) were estimated to be nearly double that of weak events (Class I), which is in agreement with the

results of Mendoza et al.'s [24] that were obtained in a coastal area in the northwest Mediterranean Sea. In addition, the magnitude of wave run-up was found to be affected by coastal morphology. More specifically, for a particular storm class, greater values of wave run-up were calculated on beach profiles with steeper slopes. Thus, the minimum values of wave run-up were calculated at the northern, northeastern, and northwestern parts of the island, which were associated with mild shoreface slopes (<4%). However, low values of run-up on gentle slope beaches are not always associated with low flood vulnerability, since the FVI depends on beach elevation as well. Due to the low beach height of the northwestern region, the vulnerability to coastal flooding was assessed as very high from weak to extreme events. As the beach slope was doubled, the representative value of wave run-up was increased by 1.2–1.5 times.

The FVI was assessed higher at upper classes. In the greatest part of the study area, vulnerability was assessed as very high for extreme storms. The FVI in the northwestern part of the study area under dissipative conditions (i.e., at Kremasti), with low beach height and gentle shoreface slope, was assessed as very high for each storm class (from weak to extreme events), and it was assumed as the most vulnerable to coastal flooding. The high vulnerability of regions with low beach altitudes and mild slopes was also noted by Kokkinos et al. [25] in two regions in the North and South Aegean Sea, as well as by Jimenez et al. [38] in three different micro-tidal environments in the Mediterranean Sea. On the other hand, according to storm analysis, the most intense events occur in the eastern and southeastern part of the study area due to strong southeast waves; however, the southeastern region was assessed as the least vulnerable to flooding during weak events. This region is characterized by great beach berm elevations and steep slopes. It was also noted that in a specific beach of great length (i.e., at the south-eastern part), the FVI may vary between the profiles due to the different beach height of the profiles.

As Garnier et al. [7] mentioned for the micro-tidal environments of the Mediterranean Sea, waves are the main factors to total water level, so tidal levels were excluded from the current analysis. On the other hand, storm surge was taken into consideration in the FVI assessment because Krestenitis et al. [39] mentioned significant sea level rise in the wider region of Rhodes Island at the Levantine–Aegean passage. To assess the worst-case scenario, the maximum value of storm surge of each storm class was taken into account for calculating the FIP index [40]. The joint occurrence of storm surge and wave heights was examined by calculating the correlation coefficient of the two parameters over the analysis period, and the correlation was found to be low to moderate, as Petroliaqkis et al. [41] also noted in various coastal areas in the Mediterranean Sea.

The wave and morphological data used in this study were mainly obtained from large-scale databases, namely Atlas, EMODnet, and Hellenic Cadastre, so the presented approach can be applied to a regional-scale preliminary analysis [12]. In the case of a local-scale analysis, it is necessary to use data from topographic surveys, and it may be useful to estimate wave run-up by using numerical models for more accurate results. In addition, as Bosom and Jimenez [11] noted, the periodically updating of morphological data after extreme storms, especially in areas where morphological changes occur, is recommended.

## 6. Conclusions

The coastal flood vulnerability assessment is an element key for coastal zone planning and management. As over the past few decades, extreme wave events have caused significant impacts on coastal regions, and there has been a growing interest for the analysis of storms and assessment of their potential hazard. This study outlines an integrated methodology for assessing coastal flood vulnerability due to wave storm events. Such an integrated approach aims to help stakeholders for a preliminary assessment of flood vulnerability at a regional scale, select measures that mitigate storm impacts, and protect coastal regions against flooding. The FVI is an index that helps decision makers to identify the most prone areas to flooding by taking both geomorphological and oceanographic components into account. In addition, as the study area is a mass touristic destination with great

potential in augmenting this economic sector, the application of the FVI is of essential interest for the local community in order to maintain the excellent tourist product.

Most intense wave storm events were identified in the eastern, southeastern, and southern parts of Rhodes Island. Regarding flooding hazard, the maximum values of wave run-up were calculated in the southeastern part of the study area where the beach face slope is steep. However, due to high beach elevation in south Rhodes, this region was characterized as less vulnerable to coastal floods than the northwestern part. Particularly, the northwestern region of study area (e.g., Kremasti) was found to be the most vulnerable, as the FVI was assessed as very high for all storm classes (from weak to extreme events) due to the low beach height. The FVI at the southeastern part was found to be very low for weak storm events and very low to very high for extreme events.

This methodology provides an approach for quantifying the flood vulnerability at a regional scale by mapping coastal areas of very high vulnerability. For further research, the FVI can be applied at the local spatial scale in regions that have been characterized by high to very high vulnerability. However, such an application requires more detailed data (e.g., from topographic and bathymetric surveys). In addition, for more accurate results, a numerical model of wave run-up can be applied at a local scale.

**Author Contributions:** Conceptualization, F.-K.G. and V.K.; methodology, F.-K.G.; validation, F.-K.G. and M.C.; formal analysis, F.-K.G. and M.C.; investigation, F.-K.G. and M.C.; resources, F.-K.G., M.C. and C.K.; data curation, F.-K.G. and M.C.; writing—original draft preparation, F.-K.G.; writing—review and editing, F.-K.G. and V.K.; visualization, F.-K.G., M.C., D.V., and V.K.; supervision, V.K.; project administration, V.K.; funding acquisition, V.K. All authors have read and agreed to the published version of the manuscript.

**Funding:** The authors acknowledge support of this work by the project “Blue Growth with Innovation and application in the Greek Seas—GLAFKI (MIS 5002438)” which is implemented under the Action “Reinforcement of the Research and Innovation Infrastructure”, funded by the Operational Programme “Competitiveness, Entrepreneurship and Innovation” (NSRF 2014–2020) and co-financed by Greece and the European Union (European Regional Development Fund). All authors have read and agreed to the published version of the manuscript.

**Acknowledgments:** The authors are grateful to two anonymous reviewers for their insightful comments that greatly improved the manuscript. F.-K. Gad is also thankful to colleagues N. Martzikos, A. Panagiotakis and D. Malliouri for fruitful conversations.

**Conflicts of Interest:** The authors declare no conflict of interest.

## References

1. Karim, M.F.; Mimura, N. Impacts of Climate Change and Sea-Level Rise on Cyclonic Storm Surge Floods in Bangladesh. *Glob. Environ. Chang.* **2008**, *18*, 490–500. [\[CrossRef\]](#)
2. Ciavola, P.; Ferreira, O.; Haerens, P.; Van Koningsveld, M.; Armaroli, C.; Lequeux, Q. Storm Impacts along European Coastlines. Part 1: The Joint Effort of the MICORE and ConHaz Projects. *Environ. Sci. Policy* **2011**, *14*, 912–923. [\[CrossRef\]](#)
3. Bertin, X.; Bruneau, N.; Breilh, J.-F.; Fortunato, A.B.; Karpytchev, M. Importance of Wave Age and Resonance in Storm Surges: The Case Xynthia, Bay of Biscay. *Ocean Model.* **2012**, *42*, 16–30. [\[CrossRef\]](#)
4. Jiménez, J.A.; Sancho-García, A.; Bosom, E.; Valdemoro, H.I.; Guillén, J. Storm-Induced Damages along the Catalan Coast (NW Mediterranean) during the Period 1958–2008. *Geomorphology* **2012**. [\[CrossRef\]](#)
5. Tsoukala, V.K.; Chondros, M.; Kapelonis, Z.G.; Martzikos, N.; Lykou, A.; Belibassakis, K.; Makropoulos, C. An Integrated Wave Modelling Framework for Extreme and Rare Events for Climate Change in Coastal Areas—The Case of Rethymno, Crete. *Oceanologia* **2016**, *58*, 71–89. [\[CrossRef\]](#)
6. Perini, L.; Calabrese, L.; Salerno, G.; Ciavola, P.; Armaroli, C. Evaluation of Coastal Vulnerability to Flooding: Comparison of Two Different Methodologies Adopted by the Emilia-Romagna Region (Italy). *Nat. Hazards Earth Syst. Sci.* **2016**, *16*, 181–194. [\[CrossRef\]](#)
7. Garnier, E.; Ciavola, P.; Spencer, T.; Ferreira, O.; Armaroli, C.; McIvor, A. Historical Analysis of Storm Events: Case Studies in France, England, Portugal and Italy. *Coast. Eng.* **2018**, *134*, 10–23. [\[CrossRef\]](#)
8. UNEP/MAP/PAP. *Protocol on Integrated Coastal Zone Management in the Mediterranean. Priority Actions Programme*; UNEP/MAP/PAP: Split, Croatia, 2008.
9. Dolan, R.; Davis, R.E. An Intensity Scale for Atlantic Coast Northeast Storms. *J. Coast. Res.* **1992**, *8*, 840–853.

10. Dolan, R.; Davis, R.E. Coastal Storm Hazards. *J. Coast. Res.* **1994**, *12*, 103–114.
11. Bosom García, E.; Jiménez Quintana, J.A. Probabilistic Coastal Vulnerability Assessment to Storms at Regional Scale: Application to Catalan Beaches (NW Mediterranean). *Nat. Hazards Earth Syst. Sci.* **2011**, *11*, 475–484. [[CrossRef](#)]
12. Di Risio, M.; Bruschi, A.; Lisi, I.; Pesarino, V.; Pasquali, D. Comparative Analysis of Coastal Flooding Vulnerability and Hazard Assessment at National Scale. *J. Mar. Sci. Eng.* **2017**, *5*, 51. [[CrossRef](#)]
13. Holman, R.A. Extreme Value Statistics for Wave Run-up on a Natural Beach. *Coast. Eng.* **1986**, *9*, 527–544. [[CrossRef](#)]
14. Nielsen, P.; Hanslow, D.J. Wave Runup Distributions on Natural Beaches. *J. Coast. Res.* **1991**, *7*, 1139–1152.
15. Stockdon, H.F.; Holman, R.A.; Howd, P.A.; Sallenger, A.H., Jr. Empirical Parameterization of Setup, Swash, and Runup. *Coast. Eng.* **2006**, *53*, 573–588. [[CrossRef](#)]
16. Hubbard, M.E.; Dodd, N. A 2D Numerical Model of Wave Run-up and Overtopping. *Coast. Eng.* **2002**, *47*, 1–26. [[CrossRef](#)]
17. Yamazaki, Y.; Kowalik, Z.; Cheung, K.F. Depth-integrated, Non-hydrostatic Model for Wave Breaking and Run-up. *Int. J. Numer. Methods Fluids* **2009**, *61*, 473–497. [[CrossRef](#)]
18. Roelvink, D.; Reniers, A.; Van Dongeren, A.P.; de van Thiel Vries, J.; McCall, R.; Lescinski, J. Modelling Storm Impacts on Beaches, Dunes and Barrier Islands. *Coast. Eng.* **2009**, *56*, 1133–1152. [[CrossRef](#)]
19. Westerink, J.J.; Luetlich, R.A.; Baptists, A.M.; Scheffner, N.W.; Farrar, P. Tide and Storm Surge Predictions Using Finite Element Model. *J. Hydraul. Eng.* **1992**, *118*, 1373–1390. [[CrossRef](#)]
20. Hubbert, G.D.; McInnes, K.L. A Storm Surge Inundation Model for Coastal Planning and Impact Studies. *J. Coast. Res.* **1999**, *15*, 168–185.
21. Mendoza, E.T.; Jiménez, J.A. Regional Vulnerability Analysis of Catalan Beaches to Storms. In Proceedings of the Institution of Civil Engineers-Maritime Engineering; Thomas Telford Ltd: London, UK, 2009; Volume 162, pp. 127–135.
22. Rangel-Buitrago, N.; Anfuso, G. An Application of Dolan and Davis (1992) Classification to Coastal Storms in SW Spanish Littoral. *J. Coast. Res.* **2011**, *64*, 1891–1895.
23. Mendoza, E.T.; Trejo-Rangel, M.A.; Salles, P.; Appendini, C.M.; Lopez-Gonzalez, J.; Torres-Freyermuth, A. Storm Characterization and Coastal Hazards in the Yucatan Peninsula. *J. Coast. Res.* **2013**, *65*, 790–795. [[CrossRef](#)]
24. Mendoza, E.T.; Jimenez, J.A.; Mateo, J. A Coastal Storms Intensity Scale for the Catalan Sea (NW Mediterranean). *Nat. Hazards Earth Syst. Sci.* **2011**, *11*, 2453–2462. [[CrossRef](#)]
25. Kokkinos, D.; Prinios, P.; Galiatsatou, P. Assessment of Coastal Vulnerability for Present and Future Climate Conditions in Coastal Areas of the Aegean Sea. In Proceedings of the 11th International Conference on Hydroscience & Engineering, Hamburg, Germany, 28 September–2 October 2014; pp. 1043–1052.
26. Martzikos, N.; Lykou, A.; Makropoulos, C.; Tsoukala, V. Cluster Analysis and Classification of Storm Events at Rethymno. *Eur. Water* **2017**, *57*, 57–62.
27. Gad, F.K.; Hatiris, G.A.; Loukaidi, V.; Dimitriadou, S.; Drakopoulou, P.; Sioulas, A.; Kapsimalis, V. Long-Term Shoreline Displacements and Coastal Morphodynamic Pattern of North Rhodes Island, Greece. *Water* **2018**, *10*, 849. [[CrossRef](#)]
28. Soukissian, T.; Hatzinaki, M.; Korres, G.; Papadopoulos, A.; Kallos, G.; Anadranistakis, E. *Wind and Wave Atlas of the Hellenic Seas*; Hellenic Centre for Marine Research: Anavyssos, Greece, 2007.
29. Copernicus Climate Change Service. Water Level Change Indicators for the European Coast From 1977 to 2100 Derived from Climate Projections. Available online: <https://cds.climate.copernicus.eu/cdsapp#!/dataset/sis-water-level-change-indicators?tab=overview> (accessed on 4 October 2020).
30. EMODnet Bathymetry Consortium. EMODnet Digital Bathymetry (DTM). *EMODnet Bathymetry* **2018**. [[CrossRef](#)]
31. Soukissian, T.; Antoniou, P.; Kapsimalis, V.; Drakopoulou, P.; Kyriakidou, H.; Panagiotopoulos, I.; Anagnostou, C. A Scientific Approach to the Constitutional Law for Seashore Delimitation in Greece. In Proceedings of the 5th National Conference of Management and Improvement on Coastal Zone, Athens, Greece, 21–24 November 2011; pp. 165–174.
32. Martzikos, N.; Afentoulis, V.; Tsoukala, V. Storm Clustering and Classification for the Port of Rethymno in Greece. *Water Util. J.* **2018**, *20*, 67–79.

33. De Michele, C.; Salvadori, G.; Passoni, G.; Vezzoli, R. A Multivariate Model of Sea Storms Using Copulas. *Coast. Eng.* **2007**, *54*, 734–751. [[CrossRef](#)]
34. Soukissian, T.H. Probabilistic Modeling of Directional and Linear Characteristics of Wind and Sea States. *Ocean Eng.* **2014**, *91*, 91–110. [[CrossRef](#)]
35. Härdle, W.; Simar, L. *Applied Multivariate Statistical Analysis*; Springer: Berlin/Heidelberg, Germany, 2007; Volume 22007.
36. Vandarakis, D.; Kyriakou, K.; Gad, F.-K.; Kapsimalis, V.; Panagiotopoulos, I.; Loukaidi, V.; Hatiris, G.A.; Sioulas, A. The carrying capacity and environmental friendly plans for future tourism development in Rhodes Island, Greece. *Eur. J. Geogr.* **2019**, *10*, 149–159.
37. Mendoza, E.T.; Jiménez, J.A. Storm-Induced Beach Erosion Potential on the Catalanian Coast. *J. Coast. Res.* **2006**, *48*, 81–88.
38. Jimenez, J.A.; Ciavola, P.; Balouin, Y.; Armaroli, C.; Bosom, E.; Gervais, M. Geomorphic Coastal Vulnerability to Storms in Microtidal Fetch-Limited Environments: Application to NW Mediterranean & N Adriatic Seas. *J. Coast. Res.* **2009**, *56*, 1641–1645.
39. Krestenitis, Y.N.; Androurlidakis, Y.S.; Kontos, Y.N.; Georgakopoulos, G. Coastal Inundation in the North-Eastern Mediterranean Coastal Zone Due to Storm Surge Events. *J. Coast. Conserv.* **2011**, *15*, 353–368. [[CrossRef](#)]
40. Idier, D.; Bertin, X.; Thompson, P.; Pickering, M.D. Interactions between mean sea level, tide, surge, waves and flooding: Mechanisms and contributions to sea level variations at the coast. *Surv. Geophys.* **2019**, *40*, 1603–1630. [[CrossRef](#)]
41. Petroligkis, T.I.; Voukouvalas, E.; Disperati, J.; Bidlot, J. Joint Probabilities of Storm Surge, Significant Wave Height and River Discharge Components of Coastal Flooding Events. *Eur. Comm. Tech. Rep.* 2016. Available online: [eu/en/joint-probabilities-of-storm-surge-significant-wave-height-and-river-discharge-components-of-coastal-flooding-events](http://eu/en/joint-probabilities-of-storm-surge-significant-wave-height-and-river-discharge-components-of-coastal-flooding-events) (accessed on 4 October 2020).

**Publisher’s Note:** MDPI stays neutral with regard to jurisdictional claims in published maps and institutional affiliations.



© 2020 by the authors. Licensee MDPI, Basel, Switzerland. This article is an open access article distributed under the terms and conditions of the Creative Commons Attribution (CC BY) license (<http://creativecommons.org/licenses/by/4.0/>).